PHILOSOPHICAL TRANSACTIONS OF THE ROYAL SOCIETY A MATHEMATICAL, PHYSICAL & ENGINEERING SCIENCES

The Distribution of Surface Concentrations of Sulphur dioxide Emitted from Tall Chimneys

D. J. Moore

Phil. Trans. R. Soc. Lond. A 1969 **265**, 245-259
doi: 10.1098/rsta.1969.0052

Phil. Trans. Roy. Soc. Lond. A. **265**, 245–259 (1969) [245]
Printed in Great Britain

The distribution of surface concentrations of sulphur dioxide emitted from tall chimneys

By D. J. Moore
Central Electricity Research Laboratories, Kelvin Avenue, Leatherhead

The observed mean values of the maximum hourly average surface sulphur dioxide concentration from generating station plumes (stack height 100 m and above) exhibit a marked dependence on wind speed. At night the lowest concentrations occur in light winds, and the concentration increases almost linearly with wind speed up to speeds of 14 m s^{-1} at stack top. In the daytime the lowest concentrations occur at about 4 m s^{-1} with a secondary maximum in light winds.

The distributions of the individual hourly average values in both light and strong winds are discussed and some practical methods for predicting these distributions are suggested.

The variations with distance from the source of the axial concentration, crosswind standard deviation and the concentration integrated across wind are discussed in terms of departures from the isotropic gaussian concentration distribution.

1. Introduction

In an earlier paper (Moore 1967*b*), SO_2 concentration measurements made at Tilbury power station during the period August 1963 to February 1964 were reported. In the same paper, the method of using a computer to plot out SO_2 concentration distributions from Tilbury and Northfleet power stations was also described. This method has been used to process the data for the period November 1964 to May 1966. In this paper the discussion will be confined to the properties of the *hourly* average SO_2 concentrations (C) as recorded over the SO_2 meter network (Lucas, James & Davis 1967; Lucas, this volume, p. 143) during this period.

Owing to difficulties with computer programs and data reading equipment, the data from some parts of this period were still not available when the analysis reported in this paper was made. They will, however, provide a useful set of randomly selected independent data for later comparison.

The most straightforward approach to the problem of estimating ground level SO_2 concentrations is to assume Gaussian profiles in the vertical and crosswind directions with appropriate values for the respective standard deviations (σ_z, σ_y). This approach was shown (Moore 1967*b*; Lucas 1967) to give reasonable estimates of the *mean* maximum concentration in strong and light winds at Tilbury, but to somewhat overestimate the mean maximum in moderate winds. Extreme concentrations were also accurately estimated if the isotropic mean values were doubled to allow for reflexion at an upper stable layer. The *individual* concentration maximum showed considerable scatter and the relation with atmospheric stability was rather complex (Moore 1967*b*; Scriven 1967).

Detailed comparison of vertical temperature gradients and surface concentrations will be discussed in other papers. Here, it is intended to discuss the mean values of the concentration in terms of the concentration expected from the simple Gaussian model, having first divided the measurements into groups of approximately equal wind speed, station load and time of day. This type of division follows closely the division suggested, for example, by Pasquill (1962), and the results are discussed in § 3.

The observations within these groups still show considerable scatter due to the effect of variations in the vertical temperature gradient and to organized convective currents. A fairly straightforward way of predicting the form of the frequency distributions within the groups in terms of two uncorrelated adjustment factors is described in § 4.

Finally, the form of the whole surface pattern (i.e. not just the maxima) is discussed in § 5 and the change in the latter with the magnitude of the maximum concentration is shown to be explicable only in terms of different functional forms for the variation of the vertical and crosswind concentration distributions with distance from the source.

2. Plant details

Both plants were operating on two stacks during this period and since it had already been demonstrated by Hamilton (1967) that the plume rise was insensitive to rate of emission of heat from the stack, it was assumed, for the purpose of assessing the effective height of the plume, that the load was equally divided between the two stacks and the two halves of the plume remained separate while they were rising, but were effectively mixed when they were recorded at the surface. Also, although there were variations in the sulphur content and calorific value of the fuel during the period, mean values were used throughout this analysis because the variations in surface concentration at a particular load and wind speed due to other meteorological factors had been shown to be many times the variation due to changes in source strength at a given load. These were about ± 10 % overall for Northfleet and ± 20 % overall for Tilbury.

Table 1 shows the relations between various parameters and the rate of generation of electricity.

Table 1. Principal notation and plant details

station	Northfleet (coal fired)	Tilbury (oil fired)
normal range of electricity generation, Q_e/MW	up to 720	up to 360
relation between heat emission (per stack) and load (total), Q_m/MW	$Q_m = Q_e/12$ (load equally divided between stacks)	$Q_m = Q_e/12$
rate of SO_2 emission, Q_N/m^3 s^{-1}, at s.t.p.	$Q = 0.8\ Q_e/600$	$Q = 0.5\ Q_e/300$
average fuel	corresponding to 1.6% sulphur coal, 23 MJ kg^{-1} (no allowance for other acid gases as around 10% SO_2 would be lost in P.F. ash)	corresponding to 3% sulphur oil 40 MJ kg^{-1} with an addition of 10% to allow for other acid gases (this allowance was also made in Moore (1967*b*))
effective plume height, H/m	$120 + 500\ \bar{Q}_m^{\frac{1}{4}}/U$	$100 + 400\ \bar{Q}_m^{\frac{1}{4}}/U$
	these correspond to the median values of H reported in Hamilton 1967 and refer to measurements made at a distance of about 1500 m downwind of the stack	
efflux velocity, W_0/m s^{-1}	$20Q_e/720$ (load equally divided between stacks)	$7.5Q_e/360$
σ_z, σ_y/m	vertical and crosswind standard deviations of concentration distributions	
wind speed, U/m s^{-1}	measured at 114 m level	averaged over 1 h
concentration C(parts/10^8 vol. vol.)	maximum value C_m	averaged over 1 h

Values with a bar over the symbol indicate mean values for a group of data; without bar, value for 1 h.

Other details of plant and instrumentation are given in Lucas, James & Davis (1967), Moore (1967*a*) and Hamilton (1967), Lucas (this volume pp. 143–145).

3. The mean value of the maximum hourly average concentration as a function of wind speed and time of day

The data were divided into ranges of wind speed of 2 m s^{-1} up to 12 m s^{-1} and all speeds above 12 m s^{-1}. They were also separated into daytime (08.00 to 17.00 h local time) and nighttime (18.00 to 07.00). Originally they were further separated into winter (October to March) and summer but there was no significant difference between these latter classes. However, the annual variation will be examined again when the full range of about four years data are processed.

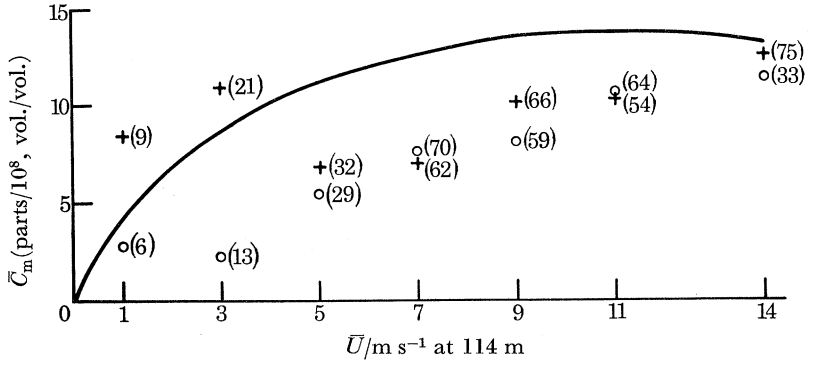

Figure 1. Mean values of the maximum hourly average concentration from Northfleet power station (mean load = 552 MW). In figures 1 to 3; + = observations between 08.00 to 17.00 h local time; ○ = 18.00 to 07.00 h local time and figures in brackets equal number of observations. The plotted curves are $\bar{C}_m = (2\bar{Q}/e\pi\bar{U}\bar{H}^2)(\frac{1}{2})$. See table 1 for method of calculation of Q, $\bar{U}$ and H.

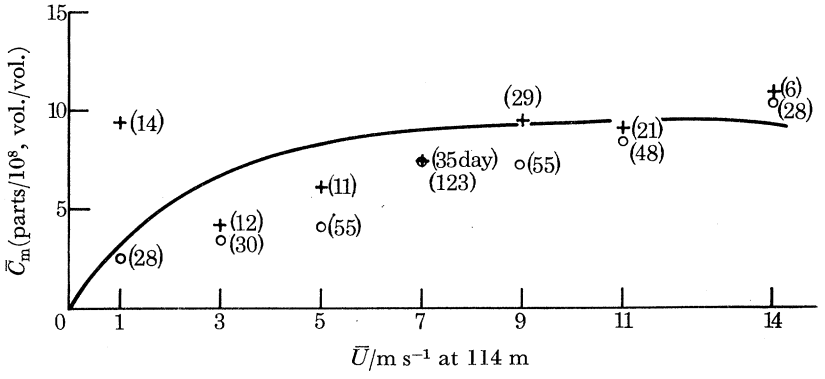

Figure 2. Mean values of the maximum hourly average concentration from Northfleet power station (mean load = 332 MW).

The data were also divided into high load Northfleet ($\geqslant$ 420 MW) medium load (120–420 MW) and high load Tilbury ($\geqslant$ 180 MW). Originally the Tilbury readings were divided into 180 to 240 MW and $\geqslant$ 240 MW because of expected downwash effects in the 180 to 240 MW range, but as there were relatively few data in this group in strong winds, this additional subdivision is not pursued here.

The mean values of the non-zero hourly average concentrations in these various groups are shown in figures 1 to 3. In these diagrams the number of hourly maxima that have been averaged to give each point are shown in brackets.

The curves plotted on figures 1 to 3 are the concentrations predicted by the continuity equation

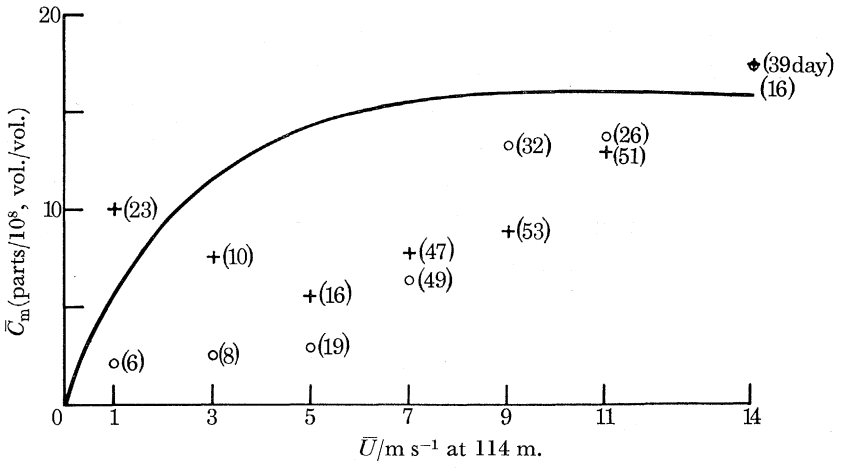

FIGURE 3. Mean values of the maximum hourly average concentration from Tilbury power station (mean load = 291 MW).

using the relations between plume height, sulphur emission, wind speed and station load given in table 1, and assuming that the ratio of vertical (σ_z/m) to horizontal (σ_y/m) spread is not a function of distance downwind and equals $\frac{1}{2}$.

The curves agree with the measured values in very strong winds (and very light winds in daytime conditions if one takes a value of σ_z/σ_y of 1 as more appropriate to those conditions). In moderate winds the measured concentrations fall below the curve.

Systematic differences between day and night conditions only become apparent in light winds, which is consistent with the Pasquill classification in which classes B and A occur only with (surface) winds of 4 m s^{-1} and below.

The assumption that σ_z/σ_y does not change with distance downwind is explicit in the Sutton type of diffusion equation and is supported more recently by Smith & Singer (1966). Other workers, notably Pasquill (1962) and Wippermann & Klug (1962) have proposed models in which σ_z/σ_y is a function of distance. By suitable choice of the disposable parameters it is possible to make this sort of equation fit the mean maxima, as indeed it is possible to fit the mean maxima by assuming that the plume continued to rise beyond the point where it was measured in the moderate winds. However, the model must also explain the features of the surface pollution pattern as a whole and this requirement is much more exacting and will be discussed in § 5.

Before we pass on to consider these patterns, for the benefit of the 'user' it is worth mentioning that a good representation of the data can be obtained by multiplying the values calculated from the homogeneous, isotropic ($\sigma_z/\sigma_y = 1$) diffusion equation (i.e. $2\bar{Q}/e\pi\bar{U}\bar{H}^2$) by an empirical correction factor ($\bar{F}$).

Day and night

Winds $\geqslant$ 4 m s^{-1} (i.e. groups in 2 m s^{-1} intervals with mean wind speeds $\geqslant$ 5 m s^{-1})

$$\bar{F} = 0.25 + 0.03(\bar{U} - 5).$$

Day (08.00 to 17.00 h) *only*

Winds $\leqslant$ 6 m s^{-1} (i.e. groups with mean speed $\leqslant$ 5 m s^{-1})

$$\bar{F} = 1 - \tfrac{1}{3}(\bar{U} - 1)^{\frac{1}{2}}.$$

Night (18.00 to 07.00 h) *only*

Winds as above

$$\bar{F} = 0.2.$$

Concentrations calculated in this simple way are compared with the measured mean values for both stations (i.e. the same data as appear in figures 1 to 3) in figure 4.

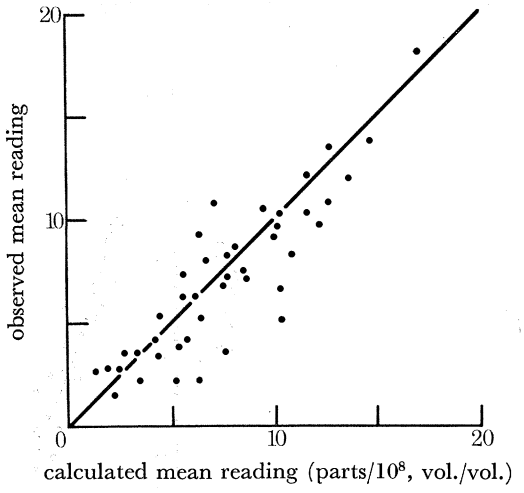

FIGURE 4. Observed concentration and concentration calculated from $\bar{C}_m = (2\bar{Q}/e\pi\bar{U}\bar{H}^2)\,\bar{F}$. All times, $\bar{F} = 0.25 + 0.03(\bar{U} - 5)$ for $\bar{U} \geqslant 5\,\mathrm{m\,s^{-1}}$; 08.00 to 17.00, $\bar{F} = 1.0 - (\bar{U} - 1)^{\frac{1}{2}}/3$ for $1 \leqslant \bar{U} \leqslant 5\,\mathrm{m\,s^{-1}}$; 18.00 to 07.00, $\bar{F} = 0.20$ for $1 \leqslant \bar{U} \leqslant 5\,\mathrm{m\,s^{-1}}$.

4. FREQUENCY DISTRIBUTIONS OF THE MAXIMUM CONCENTRATIONS AT A GIVEN WIND SPEED AND LOAD

Each of the points plotted in figures 1 to 3 represents the mean of a number of readings which showed considerable scatter. However, for each group of data represented by each of the points, it appeared that the relative frequency with which a concentration value (C'_m) was observed was a function only of C'_m divided by the value of $\bar{C}_m$ for that group, provided the light wind data were treated separately. This feature of the distributions is illustrated in figures 5 to 7. In figure 5 the Northfleet data for both load groups in the wind speed groups above $4\,\mathrm{m\,s^{-1}}$ are represented by the percentage frequency with which a given value of $C'_m/\bar{C}_m$ was exceeded. Figure 6 shows the Tilbury data for the same groups of wind speed while figure 7 shows the cumulative frequency distributions of the light wind readings for both stations.

The plotted curves were derived as follows: The *actual* observed concentration in a given hour was supposed to be equal to the concentration calculated for the homogeneous, isotropic diffusion model multiplied by two uncorrelated adjustment factors F_1 and F_2, i.e. $F = F_1 F_2$.

F_1 takes into account variations in the value of the mean plume concentration $(2Q/e\pi UH^2)$ from the value calculated from mean values of the parameters Q, U and H for the range of wind speed and station load defining the group of data considered and from errors in determining the surface concentration. That is to say that it represents departures from the expected values of the measurable parameters appearing in the diffusion equation.

F_2 takes account of the departures of the *actual* distribution of material within the plume from the twin symmetrical Gaussian distributions which would be expected if the turbulence were homogeneous and isotropic and the plume were perfectly reflected at the ground.

Values of F_1 in the range $(1 + f_1)\,\bar{F}_1$ to $(1 - f_1)\,\bar{F}_1$ were assumed to occur with equal probability and values outside this range were assumed not to occur. A similar distribution was assumed for $\bar{F}_2$ over the range $(1 - f_2)\,\bar{F}_2$ to $(1 + f_2)\,\bar{F}_2$.

The mean value of F for the group of data considered was thus equal to $\bar{F}_1\bar{F}_2 = \bar{F}$ and the probability of occurrence of a given multiple of $\bar{F}$ was determined by the values of f_1 and f_2. A more detailed discussion of the distribution is given in the appendix.

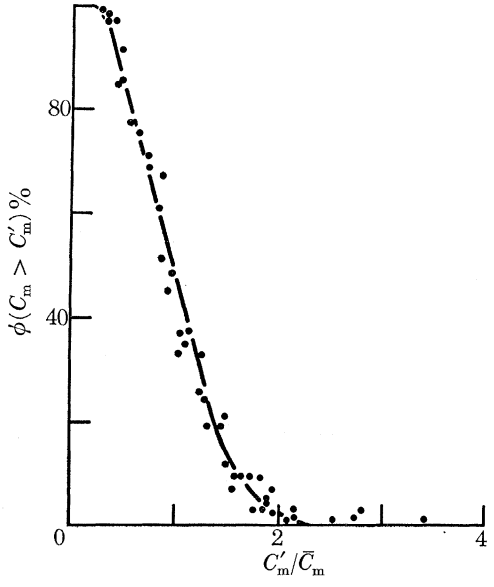

FIGURE 5. Cumulative frequency distribution Northfleet day and night readings, wind $\geqslant$ 4 m s^{-1}, divided into five groups of wind speed (as in figures 1 and 2) and two groups of load 120 to 420 MW and $>$ 420 MW.

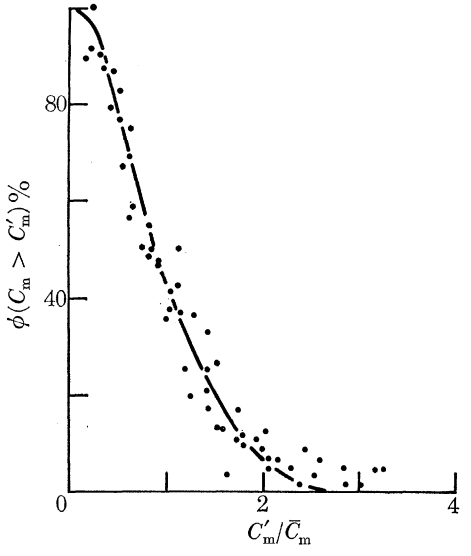

FIGURE 6. Cumulative frequency distribution: Tilbury day and night readings, winds $\geqslant$ 4m s^{-1}, divided into five groups of wind speed (as in figure 3) and two groups of load 180 to 240 MW and $>$ 240 MW

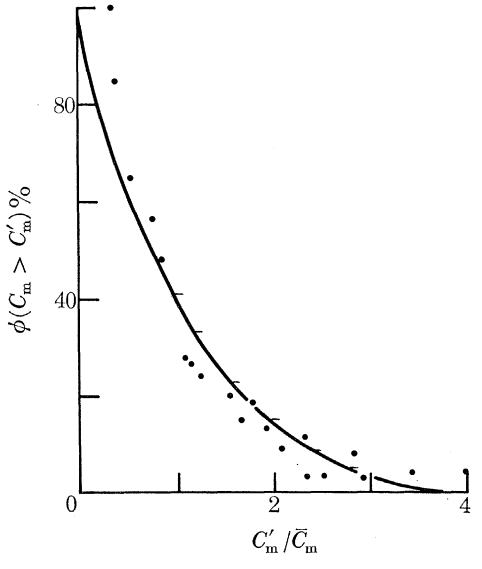

FIGURE 7. Cumulative frequency distribution Tilbury and Northfleet, all winds $<$ 4 m s^{-1} loads $\geqslant$ 180 MW Tilbury, 120 to 420 and $>$ 420 MW Northfleet day (08.00 to 17.00) readings only.

The curve in figure 5 assumes $f_1 = \frac{1}{3}$, $f_2 = \frac{5}{7}$, in figure 6, $f_1 = \frac{3}{5}$, $f_2 = \frac{5}{7}$, and in figure 7, $f_1 = 1$, $f_2 = 1$.

The scatter in plume height measurements described by Hamilton (1967), and Scriven's discussion (this volume, p. 209) of the probable effects on the value of F_2 from non-homogeneous

diffusion models indicate that $f_1 = 1$ and $f_2 = 1$ would represent about the *maximum* degree of variability that was likely. Values of f_1 near $\frac{1}{3}$ would represent the *minimum* degree of variability likely in the term $(2\bar{Q}/e\pi\bar{U}\bar{H}^2)$ from variations in fuel quality and load within the data groups, and this is the value which gives a good representation of the Northfleet data in winds over $4\,\mathrm{m\,s^{-1}}$. The larger scatter in the Tilbury data ($f_1 = \frac{3}{5}$), can probably be ascribed to the low efflux velocity (table 1) at that station, and the poorer aerodynamic characteristics, resulting in greater variability in the plume height than occurs with the Northfleet plume.

The value of $f_2 = \frac{5}{7}$ for the moderate and strong wind data for both stations probably reflects the reduced effect of solar induced convection in this group, compared with the light wind group where $f_2 = 1$.

In the above discussion we have assumed that the term showing the greater variation in strong winds was f_2. This assumption is supported by the behaviour of the surface pollution pattern as a whole, as will be demonstrated in the next section.

5. Variation of the surface pattern with observed maximum concentration

Mean surface patterns were constructed for occasions when wind speed, station load and the observed maximum concentration were roughly constant. This latter division was preferred to one of stability, because previous analysis (Moore 1967*b*) had shown that although there was a significant variation in maximum surface concentration with stability, the scatter in the individual values within a subcategory of limited stability range was still considerable. In a subsequent paper it is intended to present average stability and turbulence levels for the various groups of roughly equal maximum concentration presented here.

Within each category, the highest third of the readings for each meter where it was within a $22\frac{1}{2}°$ sector (total angle) centred about the plume axis were taken as being axial readings, i.e. readings for the centre $7\frac{1}{2}°$ of the plume. The other two-thirds were taken as readings over the two $7\frac{1}{2}°$ sectors centred $7\frac{1}{2}°$ off the plume axis.

The average crosswind standard deviation of the concentration distribution, the non-dimensional integral of concentration in the crosswind direction and the axial profile could be calculated in this way.

This method of separating into 'axial' ($\bar{C}_1$) and 'off-axis' ($\bar{C}_2$) readings was adopted because of the difficulty in defining precisely the axis of the plume because of its tendency not to lie in a straight line, and the complications caused by some of the meters being out of service.

Since the readings were very low or zero outside the $22\frac{1}{2}°$ sector except on relatively few occasions when there was a systematic shift in the wind direction during the hour considered—little error in the mean readings resulted from mistakes in placing the low readings in or out of the $22\frac{1}{2}°$ sector. Considerable errors resulted in trying to decide how near the axis of the plume a meter was in an individual hour, except on the 3.2 and 6.4 km arcs with Tilbury readings (see Moore 1967*b*), so this, the alternative method of determining the patterns, was not used.

These results are summarized in tables 2*a* to *c* which show mean values of the axial concentration ($\bar{C}_1$) at different mean distances from the source, the standard deviation of the crosswind spread (σ_y) calculated from the observed ratio of $\bar{C}_2$ and $\bar{C}_1$ for each group of data.

Also shown in tables 2*a* to *c* are the values of the normalized integrated crosswind concentration function

$$I(x) = \frac{\pi^{\frac{1}{2}} UH}{2Q} \int_{-\infty}^{+\infty} C\,\mathrm{d}y \qquad (1)$$

To ensure that a reasonable number of readings remained to average at each distance after the additional subdivision by maximum concentration, the number of wind speed groups was reduced to three, $\geqslant 8\,\mathrm{m\,s^{-1}}$, 4 to $8\,\mathrm{m\,s^{-1}}$ and $\leqslant 4\,\mathrm{m\,s^{-1}}$. Also to smooth out the peculiarities of any particular site, readings for at least two stations were averaged to give the values at each distance quoted in tables 2*a* to *c*. These distances represent the mean distance from the source considered of the sites involved.

The main features of the data are:

The *average distance downwind from the sources of the maxima* ($\bar{x}_\mathrm{m}$) appears to be very insensitive to both the magnitude of the observed surface concentration *and* the wind speed, with the exception of the high concentration, light wind readings where the high readings extend much further downwind and the distance of the maximum is difficult to define.

Tables 2*a* to *c*

In tables 2*a* to *c*, the mean concentration at meters over the central $7\frac{1}{2}°$ sector of the plume ($\bar{C}_1$), the crosswind standard deviation (σ_y) and the non-dimensional crosswind concentration integral

$$I(x) = \frac{\pi^{\frac{1}{2}} UH}{2Q} \int_{-\infty}^{+\infty} C\,\mathrm{d}y$$

are given for groups of meters at mean distance $\bar{x}$, in ranges of wind speed 0–4, 4–8 and $> 8\,\mathrm{m\,s^{-1}}$ and maximum concentration ranges R, 4 to 7, 8 to 11, etc. parts $/10^8$. Where only a few high readings were observed, the highest concentration group was taken as $\geqslant 8$, $\geqslant 12$, etc. parts/10^8. Mean loads are given for each table.

Values of $I > 0.43$ indicating possible plume reflexion are in bold type.

(*a*) Tilbury: mean load 291 MW ($\geqslant$ 180 MW)

R	$\bar{C}_1$ parts/10^8	σ_y/m	I	R	$\bar{C}_1$	σ_y	I	R	$\bar{C}_1$	σ_y	I
	$\bar{U} = 11\,\mathrm{m\,s^{-1}}$				$\bar{U} = 6\,\mathrm{m\,s^{-1}}$				$\bar{U} = 2\,\mathrm{m\,s^{-1}}$		
$\bar{x} = 10.5$ km											
4–7	1.7	1074	0.18		3.9	1000	0.36		4.0	1147	0.26
8–11	2.5	1086	0.27		4.7	769	0.33	$\geqslant 8$	20.7	985	**1.19**
12–15	3.2	911	0.29	$\geqslant 12$	3.3	1241	0.37				
16–19	3.6	809	0.29								
$\geqslant 20$	9.6	853	**0.81**								
$\bar{x} = 6.4$ km											
4–7	4.3	448	0.19		4.4	560	0.23		4.7	551	0.15
8–11	6.1	439	0.26		8.3	529	0.39	$\geqslant 8$	17.2	608	**0.61**
12–15	5.0	433	0.21	$\geqslant 12$	6.6	501	0.30				
16–19	7.6	425	0.32								
$\geqslant 20$	8.6	439	0.33								
$\bar{x} = 3.3$ km											
4–7	5.6	224	0.12		5.1	277	0.13		3.7	290	0.06
8–11	9.0	262	0.23		9.1	271	0.23	$\geqslant 8$	17.5	290	0.29
12–15	13.7	253	0.34	$\geqslant 12$	13.5	242	0.30				
16–19	18.0	292	**0.49**								
$\geqslant 20$	25.5	251	**0.63**								
$\bar{x} = 1.5$ km											
4–7	6.1	128	0.08		5.0	128	0.06		4.7	145	0.04
8–11	9.8	127	0.12		8.0	123	0.09	$\geqslant 8$	11.6	87.5	0.06
12–15	13.9	114	0.16	$\geqslant 12$	9.7	129	0.11				
16–19	17.0	133	0.22								
$\geqslant 20$	25.3	115	0.29								
	$\bar{H} = 185$ m				$\bar{H} = 246$ m				$\bar{H} = 538$ m		

(*b*) NORTHFLEET: MEAN LOAD 522 MW (⩾ 420 MW)

R	$\bar{C}_1$	σ_y	I	R	$\bar{C}_1$	σ_y	I	R	$\bar{C}_1$	σ_y	I
	$\bar{U}$ = 11 m s^{-1}				$\bar{U}$ = 6 m s^{-1}				$\bar{U}$ = 2 m s^{-1}		
$\bar{x}$ = 11.9 km											
4–7	3.8	912	0.31		3.0	932	0.20		4.7	916	0.25
8–11	3.7	892	0.29		4.8	909	0.31	⩾ 8	10.3	939	**0.56**
12–15	4.7	797	0.33	⩾ 12	8.7	778	**0.48**				
⩾ 16	3.2	874	0.25								
$\bar{x}$ = 8.2 km											
4–7	3.4	703	0.21		3.9	662	0.19		5.0	632	0.18
8–11	5.0	601	0.27		5.7	683	0.28	⩾ 8	14.1	637	**0.52**
12–15	6.7	627	0.37	⩾ 12	8.8	534	0.34				
⩾ 16	7.3	618	0.41								
$\bar{x}$ = 6.4 km											
4–7	4.7	480	0.20		3.4	531	0.13		4.0	692	0.16
8–11	6.8	419	0.28		5.8	528	0.22	⩾ 8	12.5	537	0.39
12–15	7.4	463	0.30	⩾ 12	8.3	446	0.27				
⩾ 16	7.5	465	0.31								
$\bar{x}$ = 5.2 km											
4–7	5.3	438	0.12		4.8	448	0.16		4.7	421	0.12
8–11	9.2	429	0.32		8.4	402	0.25	⩾ 8	14.8	403	0.35
12–15	12.0	424	**0.45**	⩾ 12	15.5	471	**0.53**				
⩾ 16	17.9	425	**0.66**								
$\bar{x}$ = 4.5 km											
4–7	5.8	408	0.21		5.7	416	0.17		6.0	345	0.12
8–11	9.3	380	0.32		9.0	395	0.26	⩾ 8	13.2	356	0.27
12–15	12.2	354	0.38	⩾ 12	13.8	337	0.34				
⩾ 16	17.6	332	**0.52**								
$\bar{x}$ = 3.6 km											
4–7	4.5	306	0.12		5.0	328	0.12		5.2	273	0.08
8–11	8.8	300	0.23		7.9	315	0.18	⩾ 8	6.0	367	0.13
12–15	12.1	273	0.29	⩾ 12	15.2	296	0.33				
⩾ 16	16.1	245	0.35								
	$\bar{H}$ = 244 m				$\bar{H}$ = 332 m				$\bar{H}$ = 748 m		

(*c*) NORTHFLEET: MEAN LOAD 332 MW (< 420 MW)

R	$\bar{C}_1$	σ_y	I	R	$\bar{C}_1$	σ_y	I	R	$\bar{C}_1$	σ_y	I
	$\bar{U}$ = 11 m s^{-1}				$\bar{U}$ = 6 m s^{-1}				$\bar{U}$ = 2 m s^{-1}		
$\bar{x}$ = 11.9 km											
4–7	2.5	1051	0.35		3.5	975	0.36		4.0	671	0.21
8–11	2.6	817	0.28		4.6	875	0.42	⩾ 8	9.7	1017	**0.67**
⩾ 12	5.9	863	0.68		3.7	1315	**0.51**				
$\bar{x}$ = 8.2 km											
4–7	4.0	636	0.34		3.3	689	0.24		4.4	648	0.23
8–11	4.6	553	0.34		6.0	642	0.41	⩾ 8	11.7	590	**0.55**
⩾ 12	7.8	533	**0.58**		5.4	699	0.40				
$\bar{x}$ = 6.4 km											
4–7	3.7	545	0.27		3.4	478	0.17		1.5	702	0.08
8–11	5.7	449	0.34		5.8	581	0.35	⩾ 8	12.0	439	0.42
⩾ 12	5.6	430	0.32		5.0	469	0.25				

TABLE 2*c* (*cont.*)

R	$\bar{C}_1$	σ_y	I	R	$\bar{C}_1$	σ_y	I	R	$\bar{C}_1$	σ_y	I
	$\bar{U} = 11$ m s^{-1}				$\bar{U} = 6$ m s^{-1}				$\bar{U} = 2$ m s^{-1}		
$\bar{x} = 5.2$ km											
4–7	5.9	444	0.29		5.4	425	0.24		5.4	425	0.18
8–11	8.9	420	**0.50**		7.9	449	0.37	⩾ 8	13.3	388	0.41
⩾ 12	14.7	451	**0.88**		13.2	446	**0.62**				
$\bar{x} = 4.5$ km											
4–7	5.6	415	0.31		5.7	397	0.24		4.7	409	0.15
8–11	8.5	366	0.42		8.8	385	0.36	⩾ 8	16.0	296	0.37
⩾ 12	13.3	365	**0.63**		12.2	328	0.43				
$\bar{x} = 3.6$ km											
4–7	5.1	308	0.21		5.3	316	0.18		4.0	389	0.12
8–11	7.7	283	0.30		6.3	277	0.18	⩾ 8	8.0	359	0.23
⩾ 12	11.6	282	**0.44**		14.7	250	0.39				
	$\bar{H} = 230$ m				$\bar{H} = 310$ m				$\bar{H} = 690$ m		

The actual distance is about 2.4 km for Tilbury and 4.5 km for Northfleet, and the ratio of these two distances is roughly the ratio of the squares of the source heights at about 11 m s^{-1} wind speed. We shall return to this point in the discussion of the integrated crosswind concentration function $I(x)$ below.

The fact that the mean concentration over the axial $7\frac{1}{2}°$ sector is close to the mean maximum for the group over a considerable range of distance demonstrates that the distribution of actual concentration at a point within these distance ranges (3.6 to 5.2 km Northfleet) (1.5 to 3.7 km Tilbury) can be derived quite easily from the distribution of maximum values, if the frequency of wind speeds and direction is known. Correction for off-axis wind directions can assume a gaussian distribution of standard deviation 0.08 rad (see below).

The *crosswind spread of the plume* at a given distance downwind also appears to vary but slightly with concentration or wind speed, although it is somewhat larger with light winds than with strong, and with low readings than with high. Most of the readings are fairly well represented by the simple expression $\sigma_y = 0.08x$ over the distance ranges covered in tables 2*a* to *c*. This relation lies between the Pasquill curves for categories C and D.

The fact that the σ_y values and the $\bar{x}_m$ distance do not vary very much with the magnitude of the observed maximum concentration precludes simple explanations for the departures of the observed concentrations in figures 1 to 3, namely, that these are due either to larger values of H than the lidar measurements (Hamilton 1967) at around 1500 m downwind indicated *or* to small values of (σ_z/σ_y) but with this ratio remaining independent of distance from the source. We are therefore forced to the conclusion that the differences are due to different functional relations between σ_z and distance from the source and σ_y and distance from the source or to non-Gaussian vertical distributions or both.

The *function* $I(x)$ (equation (1)) shows a very different dependence on the distance from the source in the different groups of data. However, if the data in each wind speed and load group are subdivided according to the ratio of the mean maximum concentration to the maximum concentration calculated from the simple diffusion model illustrated in figures 1 to 3, and the distance downwind is normalized to the *observed* distance of maximum concentration (i.e. the Tilbury distances are multiplied by 4.5/2.4), then a more coherent pattern emerges.

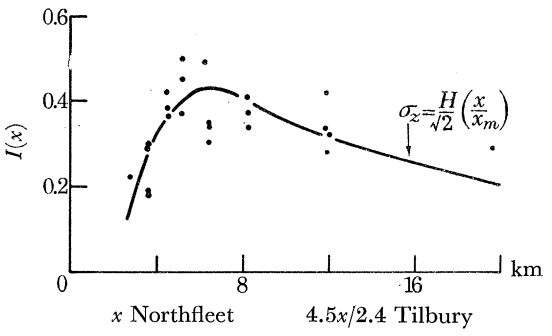

FIGURE 8. $I(x)$ as a function of x ($4.5x/2.4$ for Tilbury observations) when $\bar{C}_m \simeq (2\bar{Q}/e\pi\bar{U}\bar{H}^2)(\frac{1}{2})$.

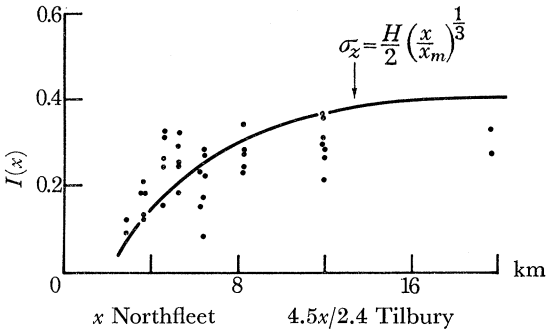

FIGURE 9. $I(x)$ as a function of x, when $\bar{C}_m \simeq (2\bar{Q}/e\pi\bar{U}\bar{H}^2)(\frac{1}{2})(\frac{1}{2})$.

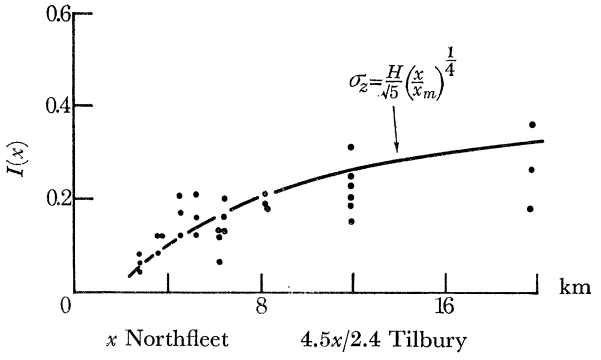

FIGURE 10. $I(x)$ as a function of x when $\bar{C}_m \simeq (2\bar{Q}/e\pi\bar{U}\bar{H}^2)(\frac{1}{2})(\frac{1}{3})$.

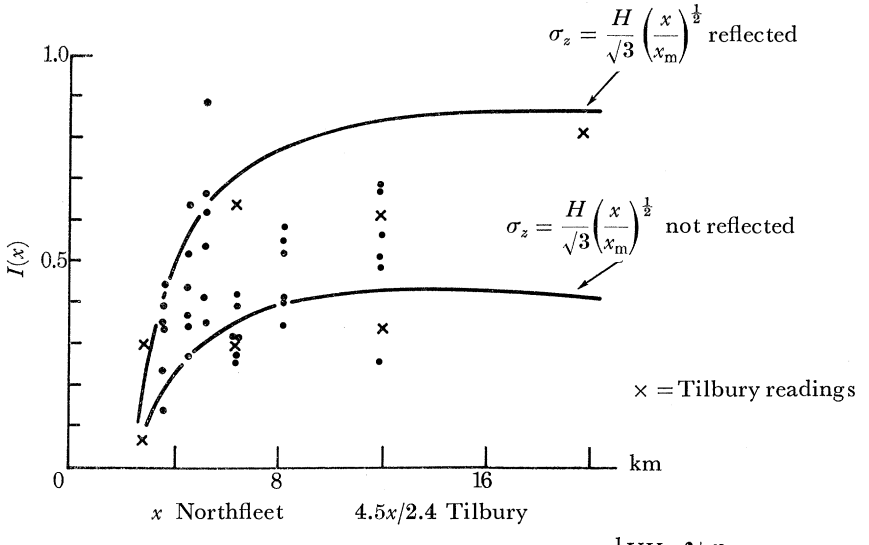

FIGURE 11. $I(x)$ as a function of x when $\bar{C}_m > (2\bar{Q}/e\pi\bar{U}\bar{H}^2)(\frac{1}{2})$. $I(x) = \frac{\pi^{\frac{1}{2}}UH}{2Q}\int_{-\infty}^{+\infty} C\,dy$.

Values of $I(x)$ as a function of distance downwind (for Northfleet plumes) and 4.5/2.4 times distance downwind for Tilbury plumes are plotted in figures 8 to 11 for groups of data where the measured maximum concentrations were approximately equal to (figure 8), approximately

one-half of (figure 9), approximately one-third of (figure 10) or were greater than (figure 11), the values expected from the curves of figures 1 to 3.

Plotted on the diagram are the curves which $I(x)$ would be expected to follow if σ_z was given by a simple power law function of x, and, as observed, $\bar{x}_m$ was independent of $\bar{C}_m$. In this case

$$\sigma_z = \frac{H}{\sqrt{(N+1)}} \left(\frac{x}{x_m}\right)^{1/N}, \tag{2}$$

$$F = \sqrt{\frac{N+1}{2\exp(N-1)}} F_*, \tag{3}$$

where F_* is the value of F when $N = 1$, i.e.

$$F_* = H/2^{\frac{1}{2}}\, 0.08 x_m \quad \text{taking } \sigma_y = 0.08x \text{ as observed.}$$

In figure 11 the top curve gives the values of $I(x)$ which would be expected if the plume were reflected at H.

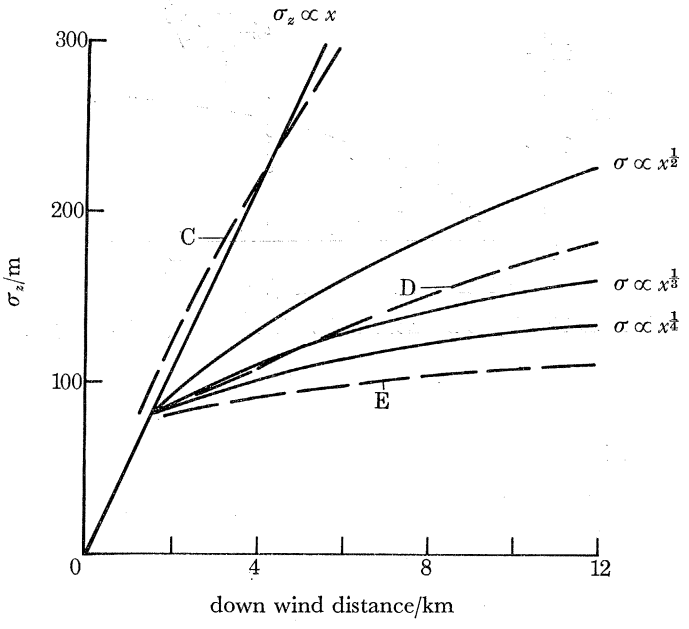

FIGURE 12. σ_z from linear, $x^{\frac{1}{2}}$, $x^{\frac{1}{3}}$ and $x^{\frac{1}{4}}$ power laws (——) compared with Pasquill E, D and C categories (— —) all plumes giving $\sigma_z \geqslant 80$ m at 1.5 km.

The general similarity between the observed values of $I(x)$ and the curves of calculated values of $I(x)$ in each of figures 8 to 11 leads one to suppose that qualitatively at least the results can be explained as follows:

(i) Where the maximum is correctly given by the simple model, the functional forms of σ_z and σ_y with distance are in fact similar. Thus a simple atmospheric model is applicable (figure 8).

(ii) When the concentration is *low* (figures 9 and 10) the plume has an initial spread at around 1 km which is always much the same (due to the fact that it is a buoyant plume), whether the vertical diffusion in the atmosphere as a whole is restricted or not. Further spread downwards may be very slow (as indicated by the low powers of x in the expressions for σ_z used to calculate the curves in these diagrams). This apparently rather odd variation of σ_z with x does in fact give a realistic representation of what might be expected to happen in these circumstances.

Figure 12 shows σ_z as a function of x calculated from equation (2) with all the plumes given a value of σ_z of 80 m at 1500 m downwind (a typical spread indicated by the lidar observations). Linear, half, third and quarter power growth curves beyond that point are then compared with the Pasquill curves for σ_z as a function of distance *downwind of the point where* $\sigma_z = 80$ m. The similarity between the curves is quite striking and illustrates the importance of the initial growth of the plume due to buoyancy when atmospheric dispersion is relatively ineffective.

(iii) If the plume has a symmetrical Gaussian distribution reflected at the surface

$$I(x) = \frac{H}{2^{\frac{1}{2}}\sigma_z} \exp \frac{-H^2}{2\sigma_z^2}$$

which has a maximum value of 0.43 (see, for example, Slade 1968, p. 349). If, however, the plume is also reflected at an upper layer, then $I(x)$ tends to 0.88 as $x \to \infty$ if the upper layer is at height H and to $0.88H^1/H$ if it is at height H^1 and the plume is entirely trapped below it.

Figure 11 therefore indicates that the high concentration plumes are often plumes trapped beneath an upper layer, because of the high values of $I(x)$ at large x. If the actual values of H had been lower than the median values for the lidar observations, then one could have expected a curve similar in shape to figure 8, but with greater values of $I(x)$. One would also have expected smaller values of x_m and a more rapid decrease in $I(x)$ with distance beyond x_m than that indicated by the curve in figure 8. Figure 11 shows that in general this was not observed on occasions with high $\bar{C}_m$.

From (i), (ii) and (iii) above it seems that we may represent the scatter in the individual values of C_m (i.e. F) at a given wind speed by a corresponding scatter in the way in which σ_z varies with distance downwind (i.e. in the values of N), and by some degree of reflexion at high values of F.

The systematic change of $\bar{F}$ with wind speed reported at the end of § 3 should therefore be interpreted as an indication of the variation in the mean value of N with wind speed. Thus $N = 1$ would represent the 'average' condition in strong winds, with some higher concentration mainly due to reflexion and some lower concentrations representing less efficient vertical diffusion. $N = 4$ would represent the 'average' condition in winds around 5 m s^{-1}.

The variation of $\bar{F}$ with wind speed does not necessarily imply a variation in the efficacy of vertical diffusion at *a given height* with wind speed, but probably represents the effect of the ratio of the height of the plume to the average height of the near neutral surface boundary layer when there is a net downward heat flux in windy conditions.

6. Conclusions

The Gaussian model of plume dispersion coupled with the plume heights calculated by the C.E.R.L. plume rise equation and $\sigma_z/\sigma_y = \frac{1}{2}$ gives estimates of the *mean* maximum hourly average surface concentration which agree with the observed values at all wind speeds within a factor of two.

The variation of the correction factor ($\bar{F}$) with wind speed and the time of day is given by simple empirical equations (§ 3). The reason for this variation probably lies in the height of the plumes relative to the mechanically stirred boundary layers and in the case of light winds to the convectively stirred boundary layer. Therefore it would be unwise to use the relations for plumes emitted from stacks with height much below 100 m. Different types of location, where the boundary layer height might be different, e.g. urban areas, might also show somewhat different relations between $\bar{F}$ and wind speed.

PHILOSOPHICAL TRANSACTIONS OF THE ROYAL SOCIETY A MATHEMATICAL, PHYSICAL & ENGINEERING SCIENCES

The distribution of individual readings could be adequately explained by ascribing the variations in F to two uncorrelated factors, one representing variations in distribution of material within the plume and the other to represent variations in the parameters determining the mean concentration in the plume. There appeared to be less variability in the latter parameter for the station with the taller stacks (Northfleet) in moderate and strong winds. Ranges of these values suggested in § 4 could be applied to similar sites subject to some modification when a wider range of observations is available.

The surface patterns were consistent with the *principal* cause of the variability in concentration being variations in the ratio of the horizontal and vertical dimensions of the plume with distance from the source and variations in the vertical profile. For practical purposes $\sigma_y = 0.08x$ appeared to represent the *average* crosswind spread in all but the lightest winds ($\leqslant 4\,\mathrm{m\,s^{-1}}$).

In winds greater than $4\,\mathrm{m\,s^{-1}}$ the distance ($\bar{x}_\mathrm{m}$) downwind of the point of maximum surface concentration was equal to about $0.075H^2\,\mathrm{m}$, where H is the plume height at $11\,\mathrm{m\,s^{-1}}$. The axial concentration was near to the maximum value from $x = \bar{x}_\mathrm{m}/\sqrt{2}$ to $x = \sqrt{2}\,\bar{x}_\mathrm{m}$ (tables 2*a* to *c*).

In lighter winds the high concentrations persisted out to the furthest readings but these were predominantly fumigation occasions with steady wind directions. The high concentrations with light variable winds in sunny convective conditions (Martin 1967) were not a noticeable factor in these observations, presumably because the sea breeze set in before these sort of conditions could become firmly established.

Point source models (see, for example, Slade 1968) indicate more variation in $\bar{x}_\mathrm{m}$ with $\bar{C}_\mathrm{m}$ than was actually observed. This appeared to be due to the rapid initial growth of the plume due to its buoyancy in conditions of relatively inefficient atmospheric dispersion in the vertical.

The methods outlined in this paper could be used to assess measurements for other sites, in particular the observations (i) that $\bar{x}_\mathrm{m}$ is not very dependent on $\bar{C}_\mathrm{m}$ in moderate or strong winds, and (ii) that the distribution of individual readings with a group of approximately equal wind speed and emission was a function of $C_\mathrm{m}/\bar{C}_\mathrm{m}$ only, could be tested where no upper air information except an estimate of wind speed was available. In this way it should be possible to obtain sets of the parameters for use in different geographical situations and different sorts of environments (urban areas, countryside, etc.). Pronounced topographical features would of course necessitate special treatment (see, for example, Hino 1968).

The author wishes to acknowledge the assistance of those members of C.E.R.L., SE Region and Computer Branch C.E.G.B. who were involved with the data acquisition and processing.

This paper is published by permission of the Central Electricity Generating Board.

References (Moore)

Hamilton, P. M. 1967 Plume height measurements at Northfleet and Tilbury power stations. *Atmos. Environment* **1**, 379–388.

Hino, M. 1968 Computer experiment on smoke diffusion over a complicated topography. *Atmos. Environment* **2**, 541–558.

Lucas, D. H. 1967 Application and evaluation of results of the Tilbury plume rise and dispersion experiment. *Atmos. Environment* **1**, 421–424.

Lucas, D. H., James, K. W. & Davis, I. 1967 The measurement of plume rise and dispersion at Tilbury power station. *Atmos. Environment* **1**, 353–366.

Martin, A. & Barber, F. R. 1967 Sulphur dioxide concentrations measured at various distances from a modern power station. *Atmos. Environment* **1**, 655–676.

Moore, D. J. 1967*a* Meteorological measurements on a 187 m tower. *Atmos. Environment* **1**, 367–378.

PHILOSOPHICAL TRANSACTIONS OF THE ROYAL SOCIETY A MATHEMATICAL, PHYSICAL & ENGINEERING SCIENCES

Moore, D. J. 1967*b* Sulphur dioxide concentration measurements near Tilbury power station. *Atmos. Environment* **1**, 389–410.
Pasquill, F. 1962 *Atmospheric diffusion*, pp. 207–210. London: Von Nostrand.
Scriven, R. A. 1967 Properties of the maximum ground-level concentration from an elevated source. *Atmos. Environment* **1**, 411–420.
Slade, D. H. 1968 *Meteorology and atomic energy*. Oak Ridge: U.S. Atomic Energy Commission.
Smith, M. E. & Singer, I. A. 1966 Atmospheric dispersion at Brookhaven National Laboratory. *Int. J. Air Wat. Pollut.* **10**, 125–135.
Wippermann, F. & Klug, W. 1962 Ein Verfahren zur Bestimmung von Schornstein Mindesthohen. *Int. J. Air Wat. Pollut.* **6**, 27–37.

Appendix

We assume that the adjustment factors F_1 and F_2 have a range of values

$$(1-f_1)\,\bar{F}_1 \leqslant F_1 \leqslant (1+f_1)\,\bar{F}_1 \quad \text{and} \quad (1-f_2)\,\bar{F}_2 \leqslant F_2 \leqslant (1+f_2)\,\bar{F}_2$$

and that the probability of any value within these ranges occurring is equal to $1/(2f_1\bar{F}_1)$ and $1/(2f_2\bar{F}_2)$ respectively and outside these ranges it is zero.

It follows that if

$$K = \frac{F}{\bar{F}_1\bar{F}_2(1+f_1)\,(1+f_2)},$$

$$y = \frac{F_2}{\bar{F}_2(1+f_2)} \quad \text{and} \quad x = \frac{F_1}{\bar{F}_1(1+f_1)},$$

then the probability that a given value of K will be exceeded is given by

$$\Phi(K) = \frac{(1-x_1)\,(1-f_2^*) - K\ln(x_2/x_1) + f_2^*(x_2-x_1)}{(1-f_1^*)\,(1-f_2^*)},$$

where

$$f_1^* = \left(\frac{1-f_1}{1+f_1}\right), \quad f_2^* = \left(\frac{1-f_2}{1+f_2}\right), \quad f_2^* \geqslant f_1^*,$$

$$x_1 = f_1^* \quad \text{when} \quad K \leqslant f_1^*, \qquad x_1 = K \quad \text{when} \quad K \geqslant f_1^*,$$

$$x_2 = K/f_2^* \quad \text{when} \quad K \leqslant f_2^*, \qquad x_2 = 1 \quad \text{when} \quad K \geqslant f_2^*.$$

This leads to the expressions for the cumulative frequency distribution and frequency density function $(-\mathrm{d}\Phi/\mathrm{d}K)$ for various ranges of K listed in table A 1.

Table A 1. The cumulative frequency $\Phi(K)$ and the frequency density function—$\mathrm{d}\Phi/\mathrm{d}K$ as a function of K where $f_1^* \leqslant f_2^*$ (i.e. $f_1 \geqslant f_2$)

range of K	$-\mathrm{d}\Phi/\mathrm{d}K$	Φ
$K \leqslant f_1^* f_2^*$	0	1
$f_1^* f_2^* \leqslant K \leqslant f_1^*$	$\dfrac{\ln(K/f_1^* f_2^*)}{(1-f_1^*)\,(1-f_2^*)}$	$\dfrac{1-f_1^*-f_2^*+K(\ln(f_1^* f_2^*/K)+1)}{(1-f_1^*)\,(1-f_2^*)}$
$f_1^* \leqslant K \leqslant f_2^*$	$\dfrac{\ln(1/f_2^*)}{(1-f_1^*)\,(1-f_2^*)}$	$\dfrac{1-f_2^*+K\ln(1/f_2^*)}{(1-f_1^*)\,(1-f_2^*)}$
$f_2^* \leqslant K \leqslant 1$	$\dfrac{\ln(1/K)}{(1-f_1^*)\,(1-f_2^*)}$	$\dfrac{1-K(1+\ln(1/K))}{(1-f_1^*)\,(1-f_2^*)}$
$K \geqslant 1$	0	0

$\Phi(K)$ = relative frequency with which the given value of K will be exceeded.

$-\dfrac{\mathrm{d}\Phi}{\mathrm{d}K}(\mathrm{d}K)$ = frequency of occurrence of values of K between K and $K+\mathrm{d}K$.

The expressions for Φ listed in table A 1 were used to plot the cumulative frequency distribution curves in figures 5 to 7.